Transition metal complexes with pyrazole based ligands. Part 27. Structural and thermal characterization of cobalt(II) halide and pseudohalide complexes with 4-acetyl-3-amino-5-methylpyrazole

VUKADIN M. LEOVAC[1*#], ZORAN D.TOMIĆ[2], KATALIN MÉSZÁROS SZÉCSÉNYI[1#], LJILJANA S. JOVANOVIĆ[1#] and MILAN D. JOKSOVIĆ[3]

[1]University of Novi Sad, Faculty of Sciences, Department of Chemistry, Trg D. Obradovića 3, 21000 Novi Sad, [2]"Vinča" Institute of Nuclear Sciences, Laboratory of Theoretical Physics and Condensed Matter Physics, P.O. Box 522, 11001 Belgrade and [3]Faculty of Sciences, University of Kragujevac, R. Domanovića 12, 34000 Kragujevac, Serbia

Abstract: The crystal and molecular structures of four tetrahedral structurally similar [Co(aamp)$_2$X$_2$] complexes (aamp = 4-acetyl-3-amino-5-methylpyrazole, X = Cl, Br, I and NCS) were determined by X-ray diffraction analysis and are discussed in detail. It was found that the different capacity of the ligand X (NCS *vs*. Cl, Br, I) for the formation of non-bonding contacts influence the mode of molecular association in the solid state. The complexes were characterized by UV–Vis spectroscopy. The first step of the thermal decomposition of the compounds was checked and is discussed in the view of the IR spectrum of the intermediate isolated from [Co(aamp)$_2$Br$_2$] by the quasi-isothermal technique.

Keywords: Cobalt(II) complexes, 4-acetyl-3-amino-5-methylpyrazole, crystal structure, electronic spectra, quasi-isothermal TA.

INTRODUCTION

Our interest in complexes with pyrazole based ligands has lasted more than a decade, due to their attractive physicochemical characteristics. Many pyrazole derivatives and their transition metal complexes exhibit biological activity, *e.g.*, derivatives of 3-aminopyrazole show anti-protozoal and cytotoxic activity.[1] Some of them are involved in enzymatic reactions.[2–4] Other 3-aminopyrazole derivatives may be used as anti-tumor agents *via* their inhibitory activity on cyclin-dependent kinase.[5–7] In order to gain a better understanding of the conditions affecting the formation of complexes, it was intended to obtain compounds in the form of single crystals with a tailored structure, by changing the experimental

---

conditions step by step. For instance, at small pyrazole molecules, the type and position of the substituents, the solvent or the temperature of the reaction mixture, as well as the central atoms and their corresponding anions were changed.[8−11] With the title ligand, 4-acetyl-3-amino-5-methylpyrazole, compounds,[12,13] including the title compounds,[14,15] have already been prepared. However, more than ten years ago there was no the possibility to determine the crystal structure of the microcrystalline title compounds. Also, the determination of their thermal decomposition was limited by the sensitivity of the available thermobalances. Now, with up-to-date equipment, it is possible to refine earlier results. Thus, in this paper, the crystal and molecular structure of $[Co(aamp)_2X_2]$ complexes (aamp = 4-acetyl-3-amino-5-methylpyrazole, X = Cl, Br, I and NCS) are reported. The discussion includes an analysis of the different potentials of X and aamp for intermolecular interactions and how they affect the association of the molecules in the solid state. On the basis of new thermal measurements, the interpretation of the first decomposition step of the compounds is also revised.

EXPERIMENTAL

Single crystals suitable for X-ray structure determination were obtained with the synthetic procedure described earlier,[14] but using more dilute solutions. Some of the physico-chemical characteristics of these compounds have been described previously.[14] In the following text the compounds $[Co(aamp)_2X_2]$ with X = Cl, Br, I and NCS are marked as **1**, **2**, **3** and **4**, respectively.

The electronic spectra for 2×10^{-3}–3×10^{-3} mol dm^{-3} methanolic solutions of the complexes were recorded on a Secomam spectrophotometer (Anthelie 2, advanced, for the spectral range 220– –900 nm) and on an FTIR instrument (NEXUS 670 FTIR, for the range 900–1400 nm).

Conductivity measurements in 1×10^{-3} mol dm^{-3} methanolic solutions of the complexes, after mild heating to complete dissolution, were performed on a digital conductivity meter, Jenway 4010.

Thermal measurements were performed using a TA Instruments SDT Q600 thermogravimetric analyzer, at a heating rate of 20 K min^{-1} in a dynamic air atmosphere (100 cm^3 min^{-1}). About 3 mg of the sample was placed in an alumina sample holder. As the reference for the DSC measurements, an identical empty alumina pan was used. For the isolation of the intermediate of the bromide compound, the SWI (quasi-isothermal[16]) mode was applied.

Crystal structure determination

The data were collected on a Bruker AXS SMART diffractometer, using MoKα radiation. The crystal structure was solved by direct methods using SIR92 software[17] and refined using the Oxford Crystals suite.[18] All non-hydrogen atoms were refined anisotropically. The hydrogen atoms were positioned geometrically at the calculated positions and allowed to ride on their parent atoms. The geometrical analysis was performed using PLATON.[19] The basic crystallographic data and structure refinement parameters are summarized in Table I.

A full list of the crystal data and refinement of **1**–**4** is deposited at the Cambridge Crystallographic Data Centre, CCDC, numbers: 655847, 655849, 655848 and 655850, respectively. They can be obtained free of charge from the Cambridge Crystallographic Data Centre *via* www.ccdc.cam.ac.uk/datarequest/cif; by post: Cambridge Crystallographic Data Centre, 12 Union Road, Cambridge CB2 1EZ, UK; by fax: +44-1223-336-033 or by e-mail: deposit@ccdc.camac.uk.

TABLE I. Selected crystallographic data and structure refinement parameters for **1**–**4**

	1	**2**	**3**	**4**
Empirical formula	$C_{12}H_{18}Cl_2CoN_6O_2$	$C_{12}H_{18}Br_2CoN_6O_2$	$C_{12}H_{18}CoI_2N_6O_2$	$C_{14}H_{18}CoN_8O_2S_2$
Formula weight	408.15	497.06	591.06	453.41
Temperature, K	293	293	293	293
Wavelength, Å	0.71073	0.71073	0.71073	0.71073
Crystal system	Monoclinic	Monoclinic	Triclinic	Monoclinic
Space group	C2/c	C2/c	P-1	Pc
a / Å	18.785(2)	19.023(1)	8.1680(5)	9.1209 (17)
b / Å	8.498(1)	8.7846(6)	10.9704(7)	7.7106 (15)
c / Å	13.952(2)	13.998(1)	11.0852(7)	14.183 (3)
α / °	90	90	97.793(1)	90
β / °	131.156(2)	131.697(2)	98.213(1)	100.800 (8)
γ / °	90	90	108.925(1)	90
Volume, Å^3	1677	1746	912	980
Z	4	4	2	2
D_c / mg m^{-3}	1.617	1.890	2.152	1.537
$F(000)$	836	980	562	466
θ range, °	3.9–30.0	2.7–34.4	1.9–30.0	2.3–30.0
Reflections collected	11174	5659	12085	3142
Independent reflections	2423	3249	5277	2968
$N_{ref.}$ [$I > 2\sigma(I)$]	1741	2267	4273	2679
$N_{par.}$	105	141	208	244
GOF (F^2)	1.00	0.87	0.93	0.93
R [$I > 2\sigma(I)$]	0.0673	0.0324	0.0378	0.037
wR (all data)	0.1673	0.0685	0.0971	0.093

RESULTS AND DISCUSSION

Molecular and crystal structures

In all four complexes, the aamp ligand is bound to the metal through the N2 nitrogen of the pyrazole ring as a neutral monodentate ligand. The pair of X anions completes the distorted tetrahedral coordination, with the ambidentate NCS bound to Co(II) in **4** through the N atom. In the crystal structure of **1** and **2**, Co(II) resides on a twofold rotation axis. The perspective view of the complexes **2** and **4**, together with the atom numbering scheme are shown in Figs. 1 and 2. Selected bond angles and bond distances are given in Tables II and III. Comparison with the related structures[12] reveals no unexpected differences in the metric parameters of the title compounds. In complexes **1**–**3,** the anion ligands participate in hydrogen bonds with one of the amino hydrogens, while the other

amino hydrogen is weakly bound to the acetyl–O. Both hydrogen bonds are intramolecular, which indicates that X plays no significant role in the association of the molecules in the crystal structure. The dotted lines in Figs. 1 and 2 depict the weak intramolecular hydrogen bonds. In **4**, only one aamp ligand shows a similar spatial relation with X, with the amine hydrogen atoms involved in weak hydrogen bonds with the acetyl–O and the thiocyanato–N (Fig. 2, Table IV). In the same complex, the second pyrazole ligand exists in its other tautomeric form, *i.e.*, as 4-acetyl-5-amino-3-methylpyrazole. To the best of our knowledge, this is the first example of the isolation of the specified tautomer of this ligand. The difference is visualized in Fig. 3, where part of **4** is overlaid compound **2**.
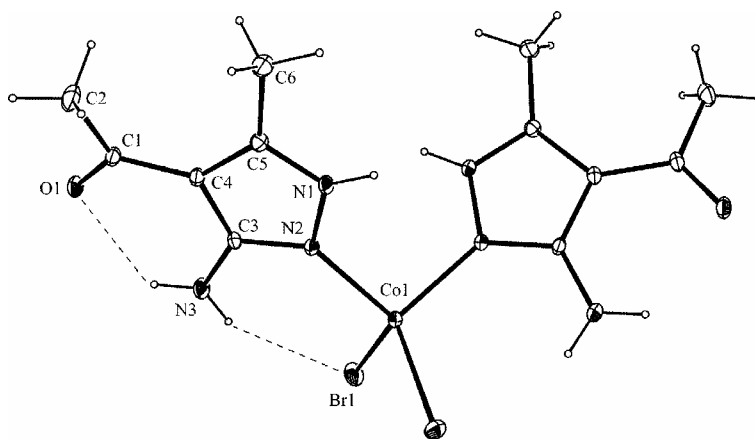

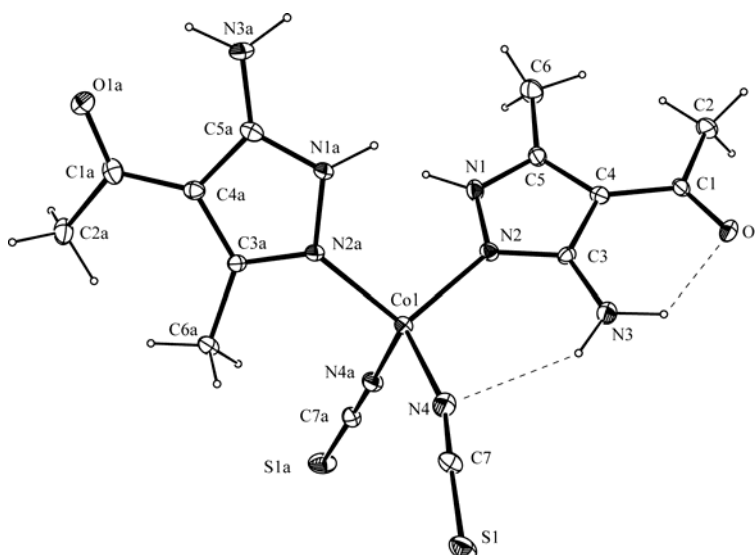Fig. 1. The molecular unit and atom numbering scheme of $[Co(aamp)_2Br_2]$.

Fig. 2. Molecular structure and atom numbering scheme of $[Co(aamp)_2(NCS)_2]$.

TABLE II. Selected bond distances (Å) for **1**–**4**

	1	**2**	**3**	**4**
N1−N2	1.374(5)	1.386(3)	1.381(5)/1.376(5)	1.376(6)/1.392(6)
N2−C3	1.338(7)	1.348(4)	1.344(5)/1.343(5)	1.332(6)/1.352(6)
N1−C5	1.320(7)	1.326(5)	1.331(5)/1.340(5)	1.327(6)/1.341(6)
C3−C4	1.417(7)	1.420(4)	1.417(5)/1.441(5)	1.442(6)/1.421(6)
C4−C5	1.393(7)	1.406(4)	1.408(5)/1.389(6)	1.399(6)/1.412(6)
C3−N3	1.360(6)	1.346(3)	1.355(6)/1.342(5)	1.357(6)/1.343(6)
C4−C1	1.449(8)	1.443(4)	1.450(5)/1.445(5)	1.446(6)/1.445(6)
C5−C6	1.495(7)	1.484(4)	1.479(6)/1.489(6)	1.495(7)/1.494(6)
C1−C2	1.501(9)	1.502(5)	1.508(7)/1.502(6)	1.520(7)/1.515(6)
C1−O1	1.239(5)	1.240(3)	1.236(5)/1.238(5)	1.230(7)/1.249(6)
Co−N2	2.006(4)	2.002(3)	2.005(3)/2.004(3)	2.000(4)/2.007(4)
Co−X	2.247(2)	2.3840(5)	2.5964(6)/2.5682(6)	1.959(5)/1.950(4)

TABLE III. Bond angles (°) subtended at Co(II). Symmetry codes: i = 1 – x, y, –1/2–z; ii = 2 – x, y, 3/2 – z

1		**2**	
Cl2−Co1−N2	117.1(1)	Br1-Co1-N2	109.98(6)
Cl2−Co1−Cl2^i	108.3(6)	Br1-Co1-Br1^{ii}	105.67(2)
Cl2−Co1−N2^i	108.5(1)	Br1-Co1-N2^{ii}	116.77(7)
Cl2i−Co1−N2	108.5(1)	Br1^{ii} -Co1-N2	116.77(7)
N2−Co1−N2^i	97.4(2)	N2-Co1-N2^{ii}	98.1(1)
Cl2i−Co1−N2^i	117.1(1)	Br1^{ii}-Co1-N2^{ii}	109.98(6)
3		**4**	
I1−Co1−I2	111.04(2)	N2−Co1−N1a	104.7(2)
I1−Co1−N2	111.5(1)	N2−Co1−N4	109.6(2)
I1−Co1−N2a	110.3(1)	N2−Co1−N4a	108.6(2)
I2−Co1−N2	108.54(9)	N1a−Co1−N4	115.7(2)
I2−Co1−N2a	112.2(1)	N1a−Co1−N4a	110.5(2)
N2−Co1−N2a	103.0(1)	N4−Co1−N4a	107.6(2)

TABLE IV. Geometry of intermolecular hydrogen bonds. Symmetry codes: i = 1/2+x,1/2–y,1/2+z; ii = 1/2+x,3/2–y,1/2+z; iii = 2–x,2–y,2–z; iv = 1–x,1–y,1–z; v = x, –1–y,1/2+z

Compound	D–H···A	H···A (Å)	D–H···A (°)
1	N1−H11···O1^i	1.85	176
2	N1−H6···O1^{ii}	1.94	176
3	N1a−H11···O1^{iii}	1.80	169
	N1−H22··· O1a^{iv}	1.86	166
4	N1−H111···O1^v	1.81	154

The chemical similarity of compounds **1**–**3** reflects itself not only in the similar molecular structure of the three complexes (Table II), but also in their similar mode of molecular association in the crystal structure. The common motif responsible for the association of the molecules in the solid state is the N−H···O hydrogen bond formed between N1 of one molecule and the acetyl–O from the neighboring molecule. The geometrical parameters relevant for these interactions

are given in Table IV. This hydrogen bond leads to the formation of molecular chains (see Fig. 4). As Fig. 4 depicts, two neighboring molecules are connected by a pair of N–H···O hydrogen bonds. In the crystal structures of complexes **1**–**3**, the closest Co(II)···Co(II) distances are 9.02, 9.00 and 8.1 Å, respectively. In **4**, the Co(II) atoms are placed closer, at a distance of 7.63 Å. The arrangement of the molecular chains into the crystal structure in **1**–**3** is governed by weak van der Waals forces. For the sake of clarity, the hydrogen atoms which are not involved in hydrogen bonds are omitted in Fig. 4. The association of the molecules in **4** in the solid state (Fig. 5) also involves the N−H···O hydrogen bond of the same type as in **1**–**3**. However, in contrast to compounds **1**–**3**, only one of the pyrazole ligands, the one with the similar spatial relation towards X, is involved in such an interaction. The other aamp ligand is oriented so that the acetyl–O is placed at a distance 3.03 Å from the S atom of the neighboring molecule. This is 0.29 Å closer than a sum of the van der Waals radius of the S and O atoms.[20] This can be an indication for an interaction between these atoms. The role of S···O contact in the association of molecules is less investigated. However, recent results reveal its role in intermolecular interactions.[21] In the crystal structure of **4**, this contact leads to the association of two molecular chains (Fig. 5).
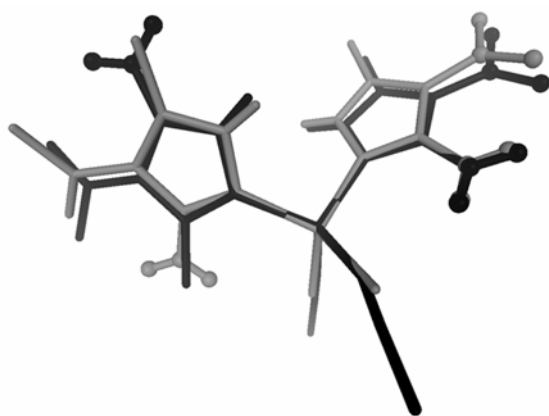

Fig. 3. Overlay of $[Co(aamp)_2(NCS)_2]$ (dark) and $[Co(aamp)_2Br_2]$ (grey) showing (left) the different orientation of the NH_2 groups (depicted as balls). Methyl hydrogens are excluded for clarity.
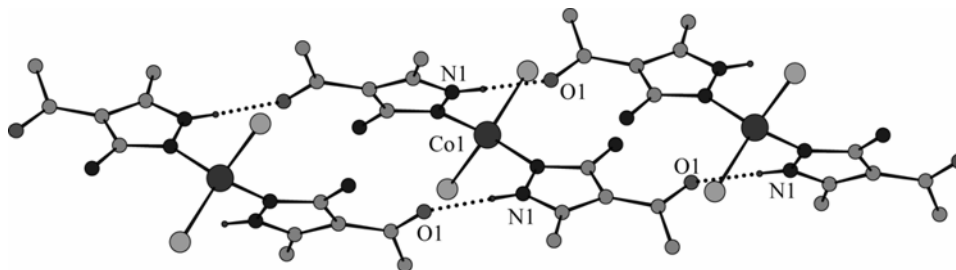

Fig. 4. Perspective view of the chain structure in $[Co(aamp)_2Br_2]$.
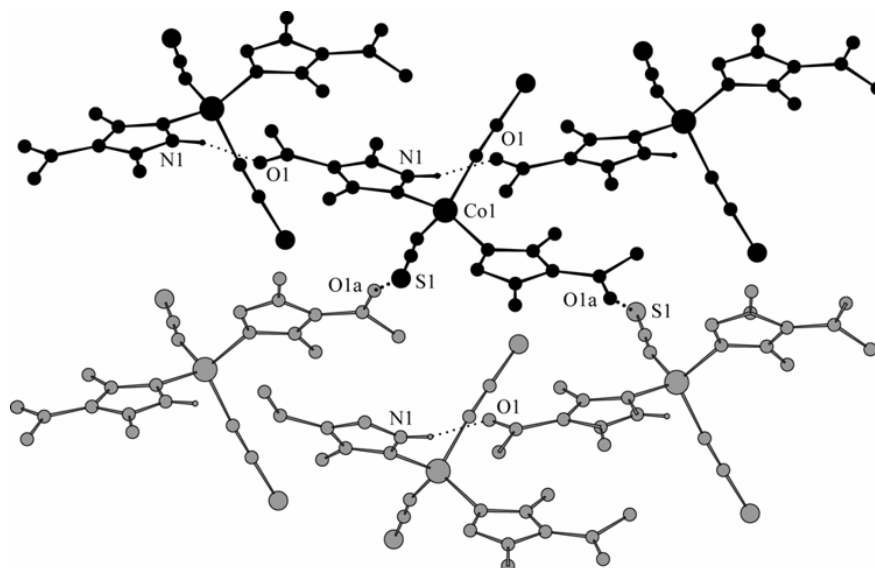
Fig. 5. Part of the crystal structure of [Co(aamp)$_2$(NCS)$_2$] showing the formation of the molecular chain driven by the hydrogen bonds and association of two chains (depicted in black and grey) governed by S···O interactions.

Conductometric and electronic spectral data

Due to the low solubility of the compounds in cold methanol, the solutions had to be mildly heated for a short time before running the UV–Vis spectra. During dissolution, the initially turquoise solutions became pink, and remained stable for days. This change of color suggests a change in the configuration from tetrahedral to octahedral, by inclusion of solvent molecules in the Co(II) coordination sphere, accompanied by the partial or complete substitution of the X ligands with solvent molecules (Table V). Namely, as can be seen from the molar conductometric data, the most stable in this respect is the NCS complex, the Λ_M of which is below the range for electrolytes of the 1:1 type (80–115 S cm^2 mol^{-1}), while the least stable is **1**, the Λ_M of which is close to that for 2:1 electrolytes (160–220 S cm^2 mol^{-1}).[22]

TABLE V. Conductometric (Λ_M) and UV–Vis (λ_{max}) spectral data of the complexes in MeOH. *sh* – Shoulder, *bp* – broad peak

Complex	Λ_M / S cm^2 mol^{-1}	λ_{max} / nm(ε / dm^3 mol^{-1} cm^{-1})
[Co(aamp)$_2$Cl$_2$]	111	241(12300), 282(10900), 482(6), 523(8), ~650*sh*(1), ~1010*bp*(2)
[Co(aamp)$_2$Br$_2$]	125	241(11700), 282(11400), 522(9), 647(2), ~1030 *bp*(3)
[Co(aamp)$_2$I$_2$]	157	< 231, 282(9500), 518(8), ~667*sh*(1), 930–1030, *bp*(9)
[Co(aamp)$_2$(NCS)$_2$]	50	240(11800), 282(10600), 488(21), 520(28), 620*sh*(5), ~910(2), 1048(5)

The electronic spectra of the complexes in methanol (Table V) display seve-ral types of characteristic absorption bands. Generally, the two highest energy absorptions of the complexes are similar to those of the ligand itself [(λ_{max}, nm, 240 (ε, dm^3 mol^{-1} cm^{-1}, 6280) and 283 (5600)[23]]. These bands are well defined and are due to intraligand transitions. Since π(ligand) $\rightarrow$ Co(II) electron transfers are also expected in this range ($\approx$ 280 nm),[24] the only slightly changed appea-rance and λ_{max} position of the band at 282 nm if compared to that of the ligand are the consequence of their weak intensity. In addition, the minor shifts in λ_{max} of both bands in the spectra of the complexes with respect to those of the ligand suggest a very loose covalency between the pyrazole ligand and Co(II).

No separate CT bands, due to X and Co(II) electron transfer were observed which, considering also the conductivity data, can be proof of their partial sub-stitution by solvent molecule in coordination with Co(II). The pink color of all the complexes in methanol and the recorded spectra for d–d interactions suggest a pseudo-octahedral geometry. For this type of high-spin d^7 complexes, three basic electron transitions occur at the levels $^4T_{2g} \leftarrow ^4T_{1g}$ (ν_1), $^4A_{2g} \leftarrow ^4T_{1g}$ (ν_2) and $^4T_{1g}$ (P) $\leftarrow ^4T_{1g}$ (ν_3).[25] A typical shape of a d–d band around ν_3 consists of a low energy shoulder and a weak, high energy absorption, as a consequence of, probably, spin–orbital coupling. The first absorption band located in the near IR range is very weak and in certain complexes rather broad (in **3** 100 nm), sugges-ting an apparent degeneracy of this level. The other transitions due presumably to trigonal distortion, which are located in the UV range, are probably either mas-ked by strong intraligand transitions or positioned out of the available range. Hence, as can be seen from the data of the spectra of most complexes, only two separate bands (ν_1 and ν_3) are observed, which can be explained in the following way. First, $^4A_{2g} \leftarrow ^4T_{1g}$ (ν_2) is a two-electron transition[25] and, therefore, relati-vely weak in intensity. Second, ν_2 and ν_3 are very close, which does not permit a precise determination of the weaker one, ν_2.

Thermal analysis

Simultaneous TG–DSC curves were recorded only up to 620 K, *i.e.*, only to obtain the first decomposition step. Namely, in a previous paper,[15] the thermal decomposition was described in detail. The sample masses used for the TA mea-surements in 1996 were about 100 mg and the heating rate was 10 K min^{-1}. All compounds showed a continuous decomposition, with a clearly separated first step. With the new up-to-date equipment, it seemed promising to isolate an inter-mediate and to characterize more closely the processes that might be involved in the decomposition. The TG curves are presented in Fig. 6.

The thermal stability increases in the following order **4 < 3 < 2 ~ 1**, as was found in a previous study.[15] However, at a higher heating rate and with a signi-ficantly lower sample mass, the thermal decomposition showed a completely

different pattern, with a much smaller mass decrease in the first step. In the case of **2**, the TG change at 560 K dropped almost to zero (see Fig. 6). The use of the quasi-isothermal (SWI) measurement mode allowed the preparation of an intermediate (Fig. 7). The mass loss corresponds to the departure of a molecule with a relative molar mass of about 39, which is much less than one HBr molecule, as was presumed earlier.[15] The FTIR spectrum of the intermediate, compared to that of the original compound is presented in Fig. 8. As can be seen, the most obvious feature of the spectra refers to demethylation of the complex (different CH_3 stretches in the range of 3000–2850 cm^{-1}, the absence of a strong CH_3 asymmetric def. + pyrazole skeleton stretch at 1492 cm^{-1} and that at 960 cm^{-1} related to C–C stretch + CH_3 rock[9]). The different bands in the 3450–2850 cm^{-1} range may also refer to the loss of an amine group. A very intensive CO stretch at 1624 cm^{-1} in the spectrum of the intermediate is still present, but shifted to a lower frequency (1600 cm^{-1}). This means that the departure of the acetyl group is excluded. Thus, the most probable decomposition mechanism may include the departure of both CH_2- and NH-groups. Obtained under the same conditions from **3**, the departing fragments have equal relative molar masses suggesting a similar decomposition pattern. However, the much higher mass loss ($M_r \approx 45$) for the chloride complex suggests a different decomposition route. This supposition is also supported by the different shape of the DTG curve of **1**. In the case of **4**, there is no way to explain the decomposition since it was not possible to isolate any intermediate. To suggest a probable decomposition mechanism, measurements using coupled TA–MS or TA–IR instruments would be necessary.[26,27]
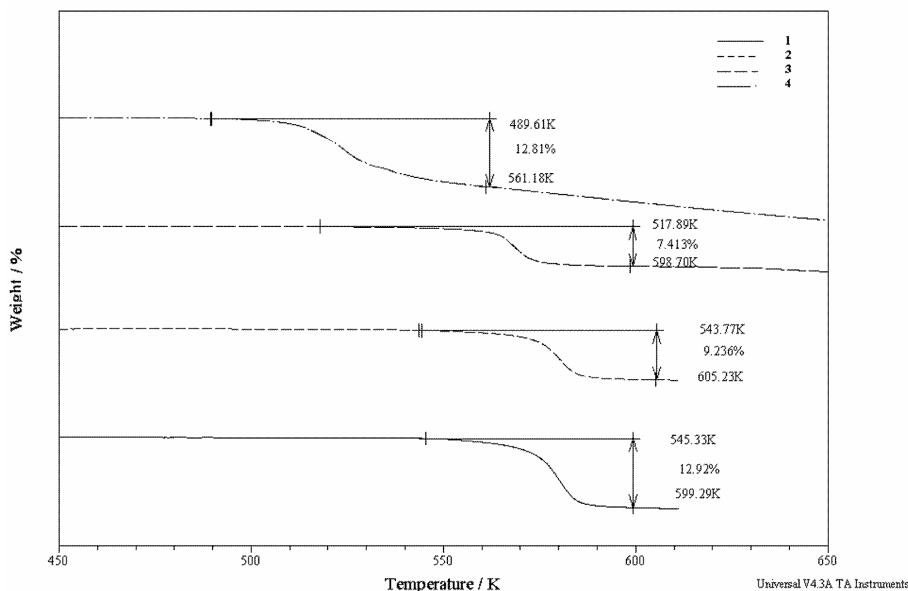

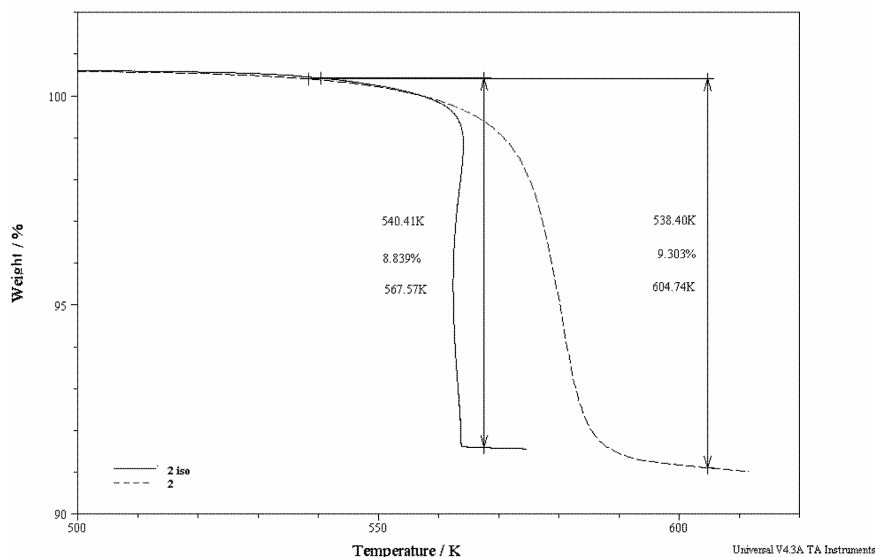Fig. 6. The first TG-step of the decomposition of **1–4**.

Fig. 7. SWI curve of **2** (—) compared with the corresponding TG (- -) curve at a heating rate of 10 K min^{-1}.

The DSC curves (Fig. 9) of the complexes for the first decomposition step give different molar enthalpy changes, ranging from 36 kJ mol^{-1} (**3**) to 25 kJ mol^{-1} for (**2**). As these values show no regularity, they cannot be used for interpretation of the processes. The peak temperatures for **1–4** are 582.8, 582.5, 570.2 and 524.7 K, respectively. No melting of the compounds during the first decomposition step was observed. The blue color of **2** changed to deep (almost black) blue for its intermediate.
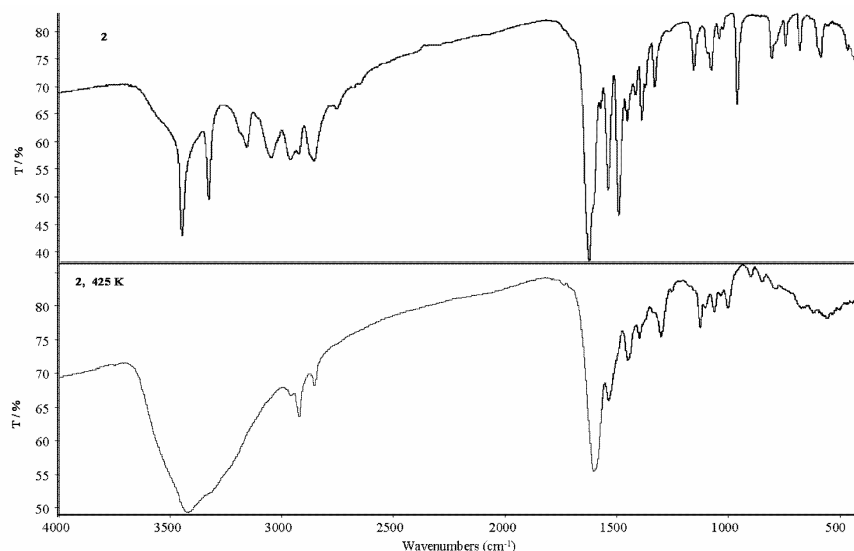

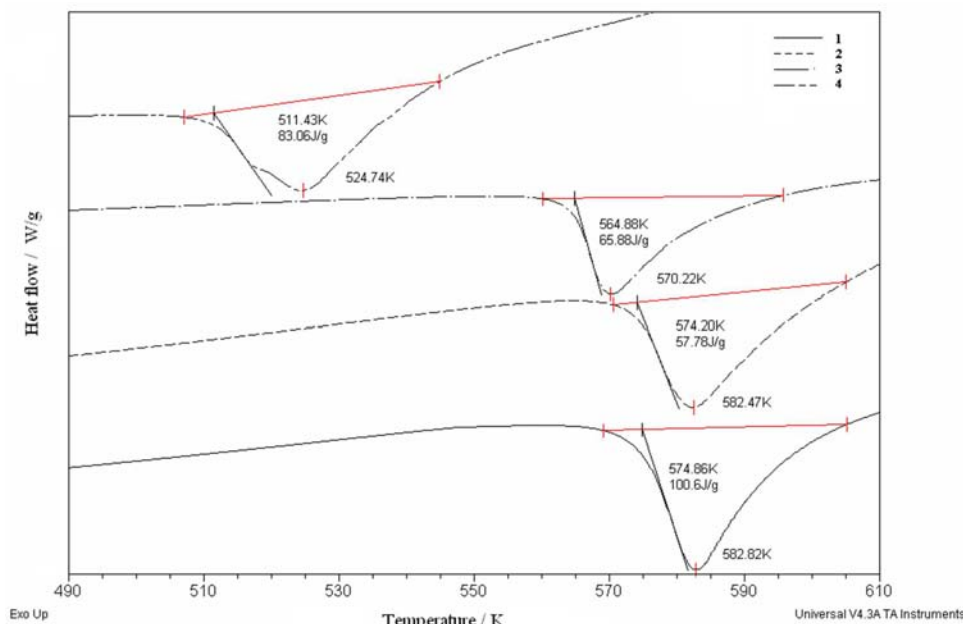Fig. 8. FTIR spectrum of **2** and the corresponding spectrum of the intermediate at 425 K.

Fig. 9. DSC curves of complexes **1**–**4**.

И З В О Д

КОМПЛЕКСИ ПРЕЛАЗНИХ МЕТАЛА СА ЛИГАНДИМА ЗАСНОВАНИМ НА ПИРАЗОЛУ. ДЕО 27. СТРУКТУРНА И ТЕРМИЧКА КАРАКТЕРИЗАЦИЈА КОБАЛТ (II) ХАЛОГЕНИДНИХ И ПСЕУДОХАЛОГЕНИДНИХ КОМПЛЕКСА СА 4-АЦЕТИЛ-3-АМИНО-5-МЕТИЛПИРАЗОЛОМ

ВУКАДИН М. ЛЕОВАЦ[1], ЗОРАН Д. ТОМИЋ[2], КАТАЛИН MÉSZÁROS SZÉCSÉNYI[1], ЉИЉАНА С. ЈОВАНОВИЋ[1] и МИЛАН Д. ЈОКСОВИЋ[3]

[1]*Департман за хемију, Природно–математички факултет, Универзитет у Новом Саду, Трг Д. Обрадовића 3, 21000 Нови Сад,* [2]*Институт за нуклеарне науке "Винча", Лабораторија за теоријску физику и физику кондензоване материје, п. пр. 522, 11001 Београд и* [3]*Природно–математички факултет, Универзитет у Крагујевцу, Р. Домановића 12, 34000 Крагујевац*

Дифракцијом X-зрака са монокристала одређене су кристалне и молекулске структуре четири врло слична тетраедарска комплекса кобалта (II) опште формуле [Co(aamp)₂X₂] (aamp = = 4-ацетил-3-амино-5-метилпиразол, X = Cl, Br, I, NCS). Утврђено је да разлике у својствима анјонских лиганада (NCS у односу на Cl, Br и I) утичу на начин груписања молекула у чврстом стању. Комплекси су окарактерисани UV–Vis спектроскопијом и методама термичке анализе, уз интерпретацију првог ступња термичког разлагања.

(Примљено 2. августа 2007)

REFERENCES

1. N. R. Sperandeo, R. Brun, *ChemBioChem.* **4** (2003) 69
2. D. R. Compton, S. Sheng, K. E. Carlson, N. A. Rebacz, I. Y. Lee, B. S. Katzenellenbogen, J. A. Katzenellenbogen, *J. Med. Chem.* **47** (2004) 5872
3. M. Suzuki, H. Iwasaki, Y. Fujikawa, M. Sakashita, M. Kitahara, R. Sakoda, *Bioorg. Med. Chem. Lett.* **11** (2001) 1285
4. M. E. Fraley, R. S. Rubino, W. F. Hoffman, S. R. Hambaugh, K. A. Thomas, *Bioorg. Med. Chem. Lett.* **12** (2002) 3537
5. S. Samanta, B. Debnath, A. Basu, S. Gayen, K. Srikanth, T. Jha, *Eur. J. Med. Chem.* **41** (2006) 1190
6. P. Pevarello, M. G. Brasca, R. Amici, P. Orsini, G. Traquandi, L.Corti, C. Piutti, P. Sansonna, M. Villa, B. S. Pierce, M. Pulici, P. Giordano, K. Martina, E. L. Fritzen, R. A. Nugent, E. Casale, A. Cameron, M. Ciomei, F. Roletto, A. Isacchi, G. P. Fogliatto, E. Pesenti, W. Pastori, A. Marsiglio, K. L. Leach, P. M. Clare, F. Fiorentini, M. Varasi, A. Vulpetti, M. A. Warpehoski, *J. Med. Chem.* **47** (2004) 3367
7. P. Pevarello, D. Fancelli, A. Vulpetti, R. Amici, M. Villa, V. Pittalà, P. Vianello, A. Cameron, M. Ciomei, C. Mercurio, J. R. Bischoff, F. Roletto, M. Varasi, M. G. Brasca, *Bioorg. Med. Chem. Lett.* **16** (2006) 1084
8. K. Mészáros Szécsényi, V. M. Leovac, A. Kovács, G. Pokol, Ž. Jaćimović, *J. Therm. Anal. Cal.* **85** (2006) 289
9. K. Mészáros Szécsényi, V. M. Leovac, V. I. Češljević, A. Kovács, G. Pokol, Gy. Argay, A. Kálmán, G. A. Bogdanović, Ž. K. Jaćimović, A. Spasojević–de Biré, *Inorg. Chim. Acta* **353** (2003) 253
10. A. Kovács, D. Nemcsok, G. Pokol, K. Mészáros Szécsényi, V. M. Leovac, Ž. K. Jaćimović, I. Radosavljević–Evans, J. A. K. Howard, Z. D. Tomić, G. Giester, *New J. Chem.* **29** (2005) 833
11. A. Kovács, K. Mészáros Szécsényi, V. M. Leovac, Z. D. Tomić, G. Pokol, *J. Organomet. Chem.* **692** (2007) 2582
12. A. Hergold–Brundić, B. Kaitner, B. Kamenar, V. M. Leovac, E. Z. Ivegeš, N. Juranić, *Inorg. Chim. Acta* **188** (1991) 151
13. V. Yu. Kukushkin, E. A. Aleksandrova, V. M. Leovac, E. Z. Ivegeš, V. K. Konovalov, *Polyhedron* **11** (1992) 2691
14. V. M. Leovac, E. Z. Iveges, V. I. Češljević, A. F. Petrović, D. M. Petrović, D. Poleti, *J. Serb. Chem. Soc.* **61** (1996) 551
15. A. F. Petrović, S. R. Lukić, D. M. Petrović, E. Z. Iveges, V. M. Leovac, *J. Therm. Anal.* **47** (1996) 879
16. J. Paulik, F. Paulik, *Simultaneous Thermoanalytical Examinations by Means of the Derivatograph*, *Comprehensive Analytical Chemistry*, Vol. XII, Thermal Analysis, W. W. Wendlandt, Adv. Ed., Elsevier, Amsterdam, Oxford, New York, 1981, p. 47
17. A. Altomare, G. Cascarano, C. Giacovazzo, A. Guagliardi, M.C. Burla, G. Polidori, M. Camalli, J. *Appl. Crystallogr.* **27** (1994) 435
18. P. W. Betteridge, J. R. Carruthers, R. I. Cooper, K. Prout, D. J. Watkin, *J. Appl. Crystallogr.* **36** (2003) 1487
19. L. Spek, *PLATON-99, Molecular Geometry Program*, University of Utrecht, The Netherlands, 1999
20. A. Bondi, *J. Phys. Chem.* **68** (1964) 441
21. Y. Nagao, S. Miyamoto, M. Miyamoto, H. Takeshige, K. Hayashi, S. Sano, M. Shiro, K. Yamaguchi, Y. Sei, *J. Am. Chem. Soc.* **128** (2006) 9722
22. W. J. Geary, *Coord. Chem. Rev.* **7** (1971) 81
23. V. M. Leovac, Z. D. Tomić, A. Kovács, M. D. Joksović. Lj. S. Jovanović, K. Mészáros Szécsényi, *J. Organomet. Chem.* (2007), doi: 10.1016/j.organchem.2007.10.018

24. J. P. Jesson, S. Trofimenko, D. R. Eaton, *J. Am. Chem. Soc.* **89** (1967) 3148
25. A. B. P. Lever, *Inorganic Electronic Spectroscopy, Part 1*, 2nd Ed., Elsevier, Amsterdam, 1967 (Russian translation)
26. D. Czakis–Sulikowska, J. Radwańska–Doczekalska, A Czylkowska, A. Markiewicz, A. Broniarczyk, *J. Therm. Anal. Cal.* **86** (2006) 327
27. J. Madarász, G. Pokol, *J. Therm. Anal.* **88** (2007) 329.